Carbohydrate Polymer Technologies and Applications 7 (2024) 100520

Contents lists available at ScienceDirect

Carbohydrate Polymer Technologies and Applications

journal homepage: www.sciencedirect.com/journal/carbohydrate-polymer-technologies-and-applications

Multifunctional xanthan gum/wood fibers based hydrogels as novel topsoil covers for forestry and agricultural applications

Alessandro Sorze *, Francesco Valentini, Matteo Burin Mucignat, Alessandro Pegoretti, Andrea Dorigato

Department of Industrial Engineering and INSTM Research Unit, University of Trento, Via Sommarive 9, 38123 Trento, Italy

ARTICLE INFO

Keywords:
Xanthan gum
Wood fibers
Hydrogels
Cross-linking
Topsoil cover
Biodegradability

ABSTRACT

This study was focused on the development of novel bio-based and biodegradable hydrogels constituted of xanthan gum (XG) reinforced with wood fibers, to be used as eco-sustainable topsoil covers (TSCs) in support of reforestation and agricultural efforts in arid conditions. At this aim, hydrogels were developed by cross-linking XG with citric acid (CA), sodium trimetaphosphate (STMP) or tannic acid (TA) at different concentrations. Samples cross-linked with CA and TA exhibited the highest dimensional stability and exceptional water absorption capability, even after multiple absorption/drying cycles. Hydrogels with 50, 60, and 100 phr of CA displayed water vapor permeance values of about $9.5{\cdot}10^{-6}$ g/(Pa·s·m^2), i.e., comparable to commercial woven PP mulching films. The average penetration resistance of the produced hydrogels was twice that of the commercial one. The presence of wood fibers in the hydrogels provided dimensional stability and minimal shrinkage after exposure to outdoor conditions for two months (15.4 % for sample with 60 phr of CA). Furthermore, after 7 months of exposure, more than 60 % of the sample mass was biodegraded. This research demonstrated the potential of xanthan gum/wood fibers based hydrogels as TSCs with superior water-regulating properties, thus offering a simple, cost-effective and scalable technology for forestry and agriculture applications.

1. Introduction

A critical concern in recent years is the efficient use of land in agriculture and forestry, closely linked to problems such as deforestation, desertification and land degradation (Mirzabaev et al., 2019; Prigent et al., 2018). Agriculture covers more than one-third of the Earth's surface and consumes approximately 85 % of the world freshwater resources (Aznar-Sánchez, Piquer-Rodríguez, Velasco-Muñoz & Manzano-Agugliaro, 2019; Foley et al., 2005). Drylands, which constitute 40 % of the continental surface, exacerbate these effects. Nowadays, various methods are employed to increase the water use efficiency in agriculture and forestry (Dennis et al., 2000; Norton, Malinowski & Volaire, 2016). One promising approach involves the use of mulching films as topsoil covers (TSCs) to improve soil and water management. These TSCs increase soil water retention and temperature, reduce moisture consumption, promote plant growth but at the same time inhibit weed growth, increase seedling survival rates and enhance crops yield (Briassoulis & Giannoulis, 2018; Kasirajan & Ngouajio, 2012; Steinmetz et al., 2016; Yang et al., 2015). However, a significant drawback is that TSCs are currently manufactured mainly from synthetic plastics like polyethylene (PE) and polypropylene (PP), contributing to the problem of microplastic pollution, since UV degradation and erosion by wind and rain results in the breakdown of these films into small pieces that can be released on the soil (Qi et al., 2018; Wang et al., 2016; Zhang et al., 2016). Moreover, removing and disposing plastic mulching films from field require additional costs and time-consuming operations (Abrusci et al., 2011). Due to the rising concerns with plastic pollution associated to the use of synthetic TSCs, biodegradable polymers are being investigated as a possible alternative, and some of them can be already found on the market. Bioplastics already used for this application are polyhydroxyalcanoates (PHAs), such as polyhydroxybutirrate (PHB) and polyhydroxyvalerate (PHV), and polylactic acid (PLA) (Gao, Xie & Yang, 2021; Merino, Zych & Athanassiou, 2022; Tian & Wang, 2020; Yang et al., 2015). Various natural polymers, including starch, alginates, chitosan, proteins, or their combinations, have been considered for the development of fully biodegradable mulching films (Kayserilioğlu, Bakir, Yilmaz & Akkaş, 2003; Menossi, Cisneros, Alvarez & Casalongué, 2021; Merino, Gutiérrez, Mansilla, Casalongué & Alvarez,

* Corresponding author.
E-mail address: alessandro.sorze@unitn.it (A. Sorze).

https://doi.org/10.1016/j.carpta.2024.100520

Available online 28 May 2024

2018; Russo, Malinconico & Santagata, 2007; Zhao, Qiu, Xu, Gao & Fu, 2017). However, many of these products exhibit inadequate mechanical and water barrier properties, and the elevated production costs limit their diffusion on the market.

Xanthan gum (XG) is one of the most promising materials for these applications, due to its biodegradability, film-forming ability, high water absorption capability and relatively low cost (Abu Elella et al., 2021; Chang et al., 2020). It is a polysaccharide obtained by *Xanthomonas campestris* in aerobic conditions from sugar cane, corn or their derivatives, and it is largely used as thickening agent in food and cosmetics. It consists of D-glucosyl, D-mannosyl and D-glucuronyl acid residues in a 2:2:1 molar ratio and variable proportions of O-acetyl and pyruvyl residues (Becker, Katzen, Pühler & Ielpi, 1998; Garcıa-Ochoa, Santos, Casas & Gómez, 2000). Due to its peculiar properties, it can be successfully applied as controlled drug delivery system (Shalviri, Liu, Abdekhodaie & Wu, 2010; Tao et al., 2016), in separation membranes (Jang, Zhang, Chon & Choi, 2015; Vatanpour et al., 2022) or in agricultural applications (mainly as soil conditioners) (Berninger, Dietz & Gonzalez Lopez, 2021; Chang, Im, Prasidhi & Cho, 2015; Sorze et al., 2023). Xanthan gum can be cross-linked in order to produce superabsorbent hydrogels able to swell in water due to their hydrophilic tridimensional network. The most promising way to cross-link XG hydrogels is through chemical methods, adding cross-linking agents such as citric acid (CA) or sodium trimetaphosphate (STMP). In both cases, an esterification reaction occurs between the cross-linking agents and the hydroxy group of the XG chains, enhancing thus mechanical stability and water resistance of the hydrogels (Patel, Maji, Moorthy & Maiti, 2020). Another interesting natural cross-linking agent is tannic acid (TA), which is particularly effective in cross-linking polysaccharides and proteins due to its phenolic groups and high molecular weight (Maiti, Maji & Yadav, 2023; Santos et al., 2018). However, no studies have been found on the development of xanthan-based hydrogels cross-linked with tannic acid.

As demonstrated in a previous work of our group (Sorze, Valentini, Dorigato & Pegoretti, 2023), to further enhance water retention and mechanical stability of xanthan-based hydrogels, fillers based on cellulose microfibers can be successfully incorporated, reaching water absorption values above 2100 %. However, cellulose microfiber-based fillers, although decreasing the volumetric shrinkage during drying compared to neat xanthan hydrogels, still undergo considerable volumetric shrinkage once used as TSC in practical applications. Moreover, they also have a high biodegradability in contact with soil (less than 3 months) and make the material too rigid. On the basis of these considerations, to provide alternatives to commercial fossil-based materials, but with adequate technical performances, the present study is meant to improve the mechanical and dimensional stability of these hydrogel formulations by changing the type of filler, i.e., by adding longer wood fibers. In particular, the aim of the work is to develop novel xanthan/-wood fibers based hydrogels and to study the effect of three different types of cross-linking agents (i.e., citric acid, sodium trimetaphosphate and tannic acid) on the morphology, water absorption, water vapor permeability and mechanical properties of the resulting materials. These optimized hydrogels could be potentially applied as multifunctional bio-based and biodegradable topsoil covers in agriculture and forestry, becoming valid alternatives to commercial products, and avoiding the use of fossil-based polymers. The newly developed mulching films, thanks to their high water-absorption capability, will be able to absorb and retain water, helping seedlings during dry periods and improving the water management in agriculture and forestry.

2. Materials and methods

2.1. Materials

Commercial xanthan gum (XG) was provided by Galeno Srl (Prato, Italy) in the form of fine powder, with purity > 91 %, molecular weight (M_W) of $1{\cdot}10^6$ g/mol, degree of pyruvate = 0.38 and degree of acetyl = 0.41. Wood fibers STEICO® Flex-036, having an aspect ratio in the range 22.5–75 mm/mm and a bulk density of 60 kg/m^3, were provided by STEICO SE (Feldkirchen, Germany). Vegetable glycerol (or glycerine) produced by Farmalabor Srl (Assago, Italy) was used as plasticizing agent in order to confer flexibility to the produced samples. It had a purity > 98 % and a M_W of 92.1 g/mol. Citric acid monohydrate (CA), with purity 99.5 % and M_W of 210.14 g/mol, was supplied by Riedel-de Haën GmbH (Seelze, Germany). Sodium trimetaphosphate (STMP) was provided by Thermo Fisher Scientific Inc. (Massachusetts, USA) in form of colorless, nontoxic powder with a density of 2.49 g/cm^3 and a M_W of 305.9 g/mol. Tannic acid (TA) was supplied by Galeno Srl (Prato, Italy), in form of a nontoxic, water-soluble powder constituted by a mix of esters of glucose with gallic acid and 3-galloilgallic acid (purity = 97 %, M_W of 1701.19 g/mol). All the materials were used as received.

2.2. Sample preparation

Samples were prepared by mixing xanthan gum, wood fibers and glycerol. Glycerol and XG were used in a 1.2:1 weight ratio, while XG and WF were mixed in a 1:1 relative weight ratio. Glycerol and XG were mixed together to obtain a paste, then hot water (T ~ 60 °C) was added to the paste and mixed for 3 min with an industrial mixer (Fama Industries Srl, Italy), until a homogeneous and lump-free solution was obtained. Wood fibers were further reduced in size using a JK-IKA LABORLINK M20 grinder for 30 s, reaching an average length of 9–30 mm, and then added to the solution. The compound was then stirred again until a homogeneous mixture was obtained. Different compositions were prepared by adding the three cross-linking agents (CA, STMP and TA), previously dissolved in 50 ml water solution at different concentrations, as reported in Table 1. A reference sample (XG_WF) without any cross-linking agent was also produced. The resulting mixtures were manually spread on a plate, dried at room temperature and then subjected to a thermal treatment of 165 °C for 3.5 min in oven, in order to perform the cross-linking reaction. These parameters and the selected cross-linking agent concentrations were identified after preliminary trials and on the basis of literature studies on xanthan hydrogels (Bueno, Bentini, Catalani & Petri, 2013; Sorze et al., 2023). Table 1 reports the code identification and the composition, in terms of phr, of the different samples obtained.

2.3. Experimental techniques

2.3.1. Fourier-Transformed infrared spectroscopy (FT-IR)

Fourier transform infrared spectroscopy (FTIR) was carried out by using a Spectrum One machine (PerkinElmer, Waltham, MA, USA) operating in attenuated total reflection (ATR) mode in the wavenumber range of 650–4000 cm^{-1} and obtaining each spectrum from the superposition of four scans. The test was conducted in order to identify the chemical composition of the produced samples and the effects of cross-linking agent concentration. Tested samples were dried in an oven at 50

Table 1
Sample coding for the prepared xanthan/wood fibers based samples.

Code	Xanthan Gum (phr)	Wood Fiber (phr)	CA (phr)	STMP (phr)	TA (phr)
XG_WF	100	100	–	–	–
CA10	100	100	10	–	–
CA50	100	100	50	–	–
CA60	100	100	60	–	–
CA100	100	100	100	–	–
STMP50	100	100	–	50	–
STMP60	100	100	–	60	–
STMP150	100	100	–	150	–
TA5	100	100	–	–	5
TA20	100	100	–	–	20
TA50	100	100	–	–	50

°C before testing.

2.3.2. Microstructural characterization

Micrographs of the surface and of the cryofractured cross-section of the samples were obtained using a field emission scanning electron microscope (FESEM) Zeiss Supra 40, operating at an accelerating voltage of 3.5 kV inside a chamber under a vacuum of 10^{-6} Torr. Prior to the observations, the samples were dried in a fan oven at 50 °C for 48 h and then coated with a thin electrically conductive Pt/Pd layer.

The density of the samples was measured to determine the total, open, and close porosity. Specifically, the theoretical density (ρ_{th}) of samples without porosity was evaluated with the rule of mixture, by knowing the density and the nominal weight fraction of each constituent, according to Equation (I)

$$\rho_{th} = \frac{1}{\sum_i \frac{W_i}{\rho_i}} = \frac{1}{\frac{W_{XG}}{\rho_{XG}} + \frac{W_{WF}}{\rho_{WF}} + \frac{W_{GLYC}}{\rho_{GLYC}} + \frac{W_{CX}}{\rho_{CX}}} \quad \text{(I)}$$

where W_{XG}, W_{WF}, W_{GLYC} and W_{CX} are the weight fractions of the xanthan gum, wood fibers, glycerol and cross-linking agents, respectively, and ρ_{XG}, ρ_{WF}, ρ_{GLYC} and ρ_{CX} their densities. ρ_{XG}, ρ_{GLYC} and ρ_{CX} were found on the technical datasheet, while ρ_{WF} was measured with a pycnometer, as reported hereafter for the apparent density.

The apparent density (ρ_{app}), which identifies the volume together with only the closed porosity, was measured using an AccuPyc 1330 helium pycnometer (Micromeritics Instrument Corporation, GA, USA). For every composition, a disk specimen with a diameter of ~8 mm and thickness of ~3 mm was tested and inserted in a chamber with a volume of 1 cm^3. Every measurement was collected at a constant temperature of 23 °C, and 99 measurements were performed for each specimen.

The bulk density (ρ_{bulk}), which comprises both the open and the closed porosity, was calculated as the ratio between the mass and the volume of disk specimens with a diameter of 15 mm and thickness of ~ 3 mm. The dimensions of the specimens were measured with a digital caliper and the mass with an analytical balance. Three specimens were measured for each composition.

Finally, the total porosity P_{tot}, the open porosity $P_{open}$and the close porosity P_{closed}were calculated according to Equations (II), (III) and (IV)

$$P_{tot} = 1 - \frac{\rho_{bulk}}{\rho_{th}} \quad \text{(II)}$$

$$P_{open} = 1 - \frac{\rho_{bulk}}{\rho_{app}} \quad \text{(III)}$$

$$P_{closed} = P_{tot} - P_{open} = \rho_{bulk}\left(\frac{1}{\rho_{app}} - \frac{1}{\rho_{th}}\right) \quad \text{(IV)}$$

2.3.3. Evaluation of the water absorption capacity

Water uptake tests were carried out in order to determine the behavior of produced samples under extreme flood conditions. For each sample three specimens, approximately 3 × 5 cm^2 in size and thickness ~3 mm, were placed in a container filled with 2–3 cm of water and left immersed. Mass variation due to water absorption or hydrogel swelling was recorded over time after removing periodically specimens from water. Water uptake (WU), or swelling degree, of the samples was obtained according to Equation (V)

$$WU\% = \frac{M_t - M_0}{M_0} \cdot 100 \quad \text{(V)}$$

where M_0 is the initial mass of the sample and M_t is the sample mass at the time *t*. The test was carried out until complete rupture of the specimens or after a plateau in the absorption curve was reached. Then, fully wet samples were left to dry at RT conditions. All specimens were subjected to three water absorption/desorption cycles, in order to investigate their behavior on a longer time scale. In order to understand the diffusion mechanism of water molecules through the hydrogels structure, the diffusional coefficient *n* was evaluated, according to Equation (VI) (Langer & Peppas, 1981)

$$\frac{M_t}{M_e} = kt^n \quad \text{(VI)}$$

where M_t and M_e are the masses of water absorbed at a given time *t* and at equilibrium condition, respectively, and *k* is a constant. For values of *n* equal to 0.5 the diffusion mechanism is Fickian and the diffusion of water molecules within the matrix is not characterized by any physical or chemical interaction between the liquid and the solid phases.

2.3.4. Evaluation of the water vapor permeability

Water vapor permeability (WVP) is a very important property for mulching films because it affects the soil water preservation. This analysis was performed in accordance to ASTM E96 standard. For each sample two circular specimens (diameter ~4 cm, thickness ~3 mm) were placed on a small glass container filled with 20 ml of distilled water. Vases were closed with a lid presenting a circular hole with a diameter of 1.6 cm and sealed with Parafilm®. A commercial woven polyethylene (PP) mulching film (Rama S.p.A, RE, Italy) was also tested as a reference for this experiment (0.25 mm of thickness). Specimens were placed in a climatic chamber at 30 °C and 50 % RH. Their mass was measured at regular time intervals over the span of two days. The water vapor permeance (WVP2) of the tested specimens was thus obtained through Equation (VII)

$$WVP2 = \frac{\Delta M}{tA} \cdot \frac{1}{\Delta p} \quad \text{(VII)}$$

where ΔM is the mass variation, A is the exposed area, t is the time over which ΔM occurs, while Δp is the differential water vapor pressure across the sample. It is important to emphasize that WVP2 is not water vapor permeability (usually indicated as WVP). On the contrary, it is a thickness-independent parameter and therefore allows a better comparison between inhomogeneous samples. From WVP2 it was possible to calculate the water vapor permeability (WVP) according to Equation (VIII)

$$WVP = WVP2 \cdot d \quad \text{(VIII)}$$

where d is the sample thickness. The measured WVP values were corrected for the resistance due to the still air layer and the resistance offered by the specimen surface, according to ASTM E96 standard specifications.

2.3.5. Evaluation of the penetration resistance

Penetration resistance tests were performed to simulate the resistance offered by mulching films against weed perforation. The tests were carried out according to ASTM F1306 standard with an INSTRON 5969 machine operating at 25 mm/min and equipped with a load cell of 100 N. The specimens were fixed with an appropriate sample clamping device and were perforated by a 3.2 mm diameter hemispherical probe. The maximum load to perforate the sample was determined and compared with that of a commercial woven PP mulching film. For each sample, five specimens with equal dimensions (76 × 76 × 3 mm^3) were tested.

2.3.6. Weather conditioning in external environment

Weather conditioning tests in outside environment were carried out in order to qualitatively evaluate the dimensional stability and the biodegradability of produced hydrogels. A rectangular area of the garden in the Department of Industrial Engineering of Trento University (46.06° N, 11.15° E, altitude 398 m asl) was cleared from grass and weeds, then the selected samples (discs 16 cm in diameter, thickness ~3 mm) were laid on it at a distance of ~20 cm from one another. Fig. 1 shows the weather conditions recorded during these tests.

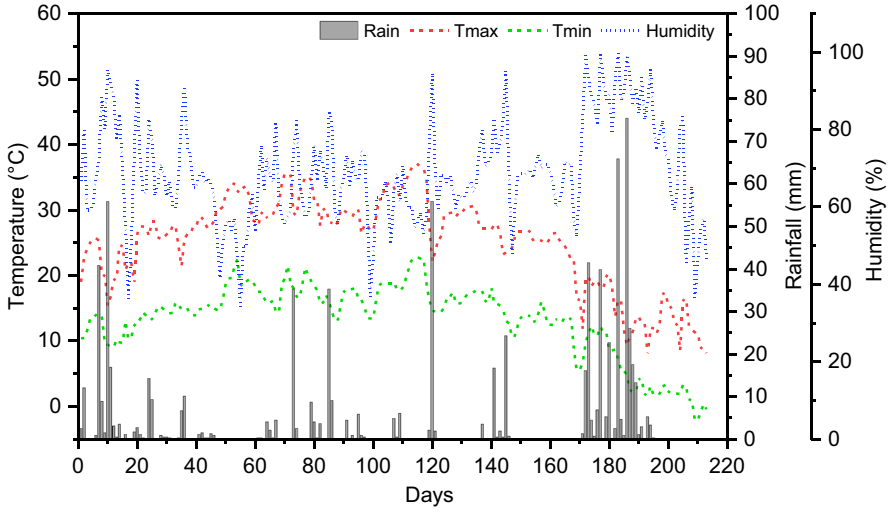

Fig. 1. Meteorological pattern recorded during open field experiments. Day 0 corresponds to May 15th 2023.

The percentage of area lost over time (A_L) due to the exposure to outside weather conditions was evaluated according to Equation (IX)

$$A_L = \frac{A_0 - A_i}{A_0} \cdot 100 \quad \text{(IX)}$$

where A_0 and A_i are, respectively, the initial area and the area at time "i" of the specimens. The area of the specimens was measured after a period of 1, 3 and 7 months. At the end the experiments the samples residues were collected, washed gently to remove attached soil, dried and weighed so that to calculate their residual mass. Only two specimens were considered, i.e., CA60 and TA5, as they proved to be most

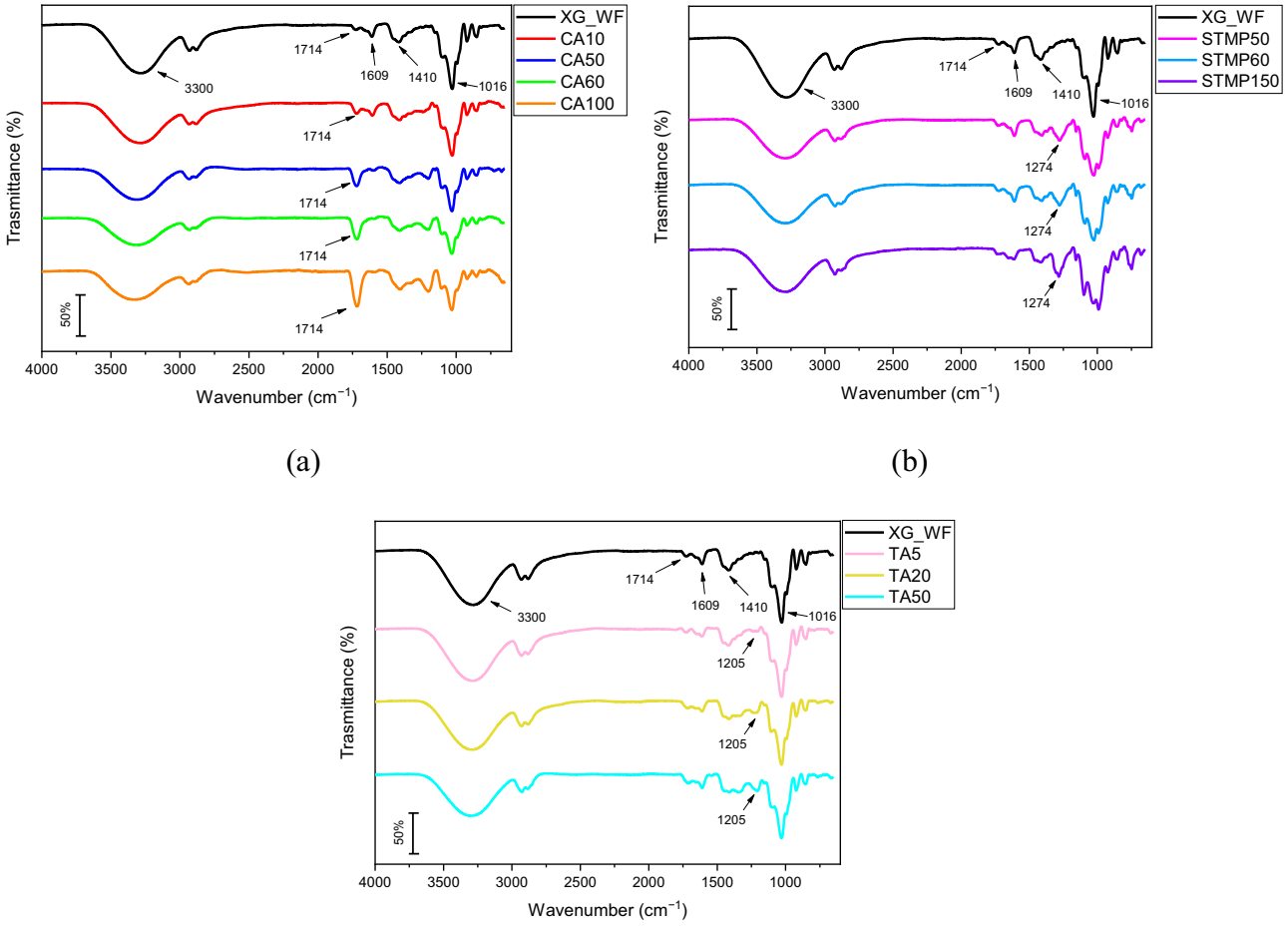

Fig. 2. FTIR spectra of XG/wood fibers samples cross-linked with different concentrations of (a) CA, (b) STMP and (c) TA.

promising compositions in terms of water absorption after multiple cycles, water vapor permeability and penetration resistance compared to the other concentrations of CA and TA, respectively. The test was also useful to qualitatively observe the ability of the samples to block weed growth, which is an important requirement for topsoil covers.

2.3.7. Statistical analysis

All the results have been presented as mean±standard error of the mean. Data of porosity, water absorption capacity, penetration resistance and weather conditioning in external environment were analyzed by using one-way analysis of variance (ANOVA) with significance level of 0.05. Pairwise differences between treatments were assessed using the post hoc Tukey's test.

3. Results and discussions

3.1. Fourier-Transformed infrared spectroscopy (FT-IR)

Fig. 2(a–c) present the FTIR spectra of the cross-linked samples with CA, STMP and TA and compare them with the reference sample (XG_WF).

For all the samples the broad absorption peak visible at 3300 cm^{-1} is ascribed to the O—H stretching vibration of hydroxyl groups, while the absorbance peak at 1016 cm^{-1} is associated to the C—O stretching vibration of the primary alcohol in XG and wood fibers. Peaks at 1410 and 1609 cm^{-1} are ascribed to the symmetrical and asymmetrical C═O vibration of the carboxylate anion (-COO^{-}), respectively, while absorbance peak at 1714 cm^{-1} is due to the presence of carbonyl groups of the carboxylic acid (-COOH) in XG and wood fibers. From Fig. 2a it can be observed that the intensity of the absorbance peak at 1609 cm^{-1} gradually decreases with the concentration of cross-linking agent, while the intensity of the peak at 1714 cm^{-1} increases. This could suggest an increase in the cross-linking degree, since more ester groups are present in the chemical structure after the esterification reaction between citric acid and xanthan gum (Li et al., 2019). In Fig. 2b samples cross-linked with STMP show an absorbance peak between 1250 and 1300 cm^{-1} whose intensity increases with the cross-linking agent content, this peak corresponds to the P═O stretching vibrations occurring from the reaction between STMP and XG and it is characteristic of the cross-linked polysaccharides (Shalviri et al., 2010). From Fig. 2c it can be noticed that the spectra of the TA cross-linked samples are very similar to that of the XG_WF sample. However, rising the TA content it is possible to observe an increase in the intensity of the peak at 1205 cm^{-1}, which can be associated to the C—O stretching vibration of the carbonyl groups of the aromatic esters of the tannic acid (Wahyono, Astuti, Gede Wiryawan, Sugoro, & Jayanegara, 2019).

3.2. Microstructural characterization

SEM micrographs of the surface and of the cross-section of a dried xanthan/wood fibers-based hydrogel are shown in Fig.. 3(a and b). Since no morphological differences were found between the samples produced, only the micrographs of the reference sample (XG_WF) were reported.

Fig. 3a clearly shows that the surface of hydrogels is constituted by a network of wood fibers coated with xanthan gum. The result is a compact surface with few macropores. From Fig. 3b it can be seen that the cross-section is characterized by lots of voids with dimensions ranging from 500 μm up to 10 μm. The presence of several pores facilitates the penetration and diffusion of water into the hydrogel network, resulting in a higher swelling capacity. Once in contact with water, the macropores fill with water first, resulting in a high initial water absorption rate. The micropores are then gradually filled, causing the hydrogel to absorb even more water (Thombare et al., 2018). It is also possible to clearly distinguish the cross-section of the wood fibers, consisting of lumens between 20 μm and 1 μm in size. These channels may improve the water storage capability of the hydrogels and increase their stiffness due to the formation of an intertwined network consisting of wood fibers.

In Table 2 the values of theoretical density, apparent density, total and open porosity of the produced hydrogels, calculated according to Equations (I), (II) and (III), are reported.

From Table 2 it can be observed that the prepared samples are

Table 2
Values of density and porosity of the xanthan/wood fibers based samples.

Sample	ρ_{th} (g/cm^3)	ρ_{app} (g/cm^3)	P_{tot} (%)	P_{open} (%)
XG_WF	1.38	1.01 ± 0.02	73.3 ± 1.5	63.2 ± 4.7
CA10	1.39	1.16 ± 0.01	76.9 ± 2.2	72.4 ± 7.4
CA50	1.40	1.19 ± 0.01	77.2 ± 1.4	73.1 ± 5.2
CA60	1.40	1.22 ± 0.01	75.8 ± 1.1	72.1 ± 3.8
CA100	1.41	1.21 ± 0.02	74.6 ± 1.2	70.3 ± 4.5
STMP50	1.47	1.13 ± 0.02	74.9 ± 2.0	67.3 ± 6.6
STMP60	1.49	1.21 ± 0.02	71.1 ± 1.3	64.3 ± 4.1
STMP150	1.61	1.39 ± 0.01	70.8 ± 1.1	66.3 ± 3.0
TA5	1.39	1.12 ± 0.02	69.1 ± 0.9	61.7 ± 2.8
TA20	1.41	1.11 ± 0.02	75.9 ± 2.1	69.3 ± 7.4
TA50	1.45	1.07 ± 0.01	75.2 ± 1.4	66.5 ± 4.3

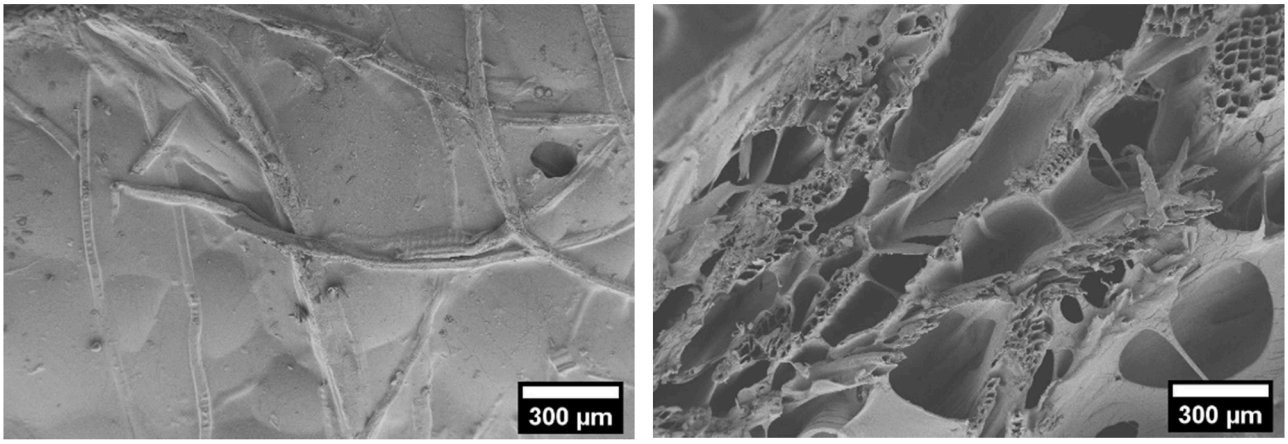

Fig. 3. SEM micrographs of dried XG_WF hydrogel, (a) surface and (b) cross-section.

characterized by total porosity values ranging from 69 % to 77 %, with no difference at significance level of 0.05. Therefore, there is no clear influence of the type and content of cross-linking agent on the porosity. In particular, hydrogels are mainly characterized by an open porosity formed during the mixing phase in the production process, where air bubbles develop in the xanthan-based solution. Moreover, the introduction of wood fibers further contributes to increase the formation of pores in the structure, which can positively influence the final water absorption capability of the produced samples, but can also negatively affect their mechanical properties.

3.3. Evaluation of the water absorption capacity

Fig. 4(a–c) shows the water absorption curves of XG_WF sample and of the hydrogels cross-linked with CA, STMP and TA.

All the tested specimen are able to reach a water uptake (WU) plateau and to resist in immersion for 8 days. The fact that the reference sample is insoluble in water and reaches a plateau (1300 %) confirms that an esterification reaction between the xanthan acid groups (pyruvyl or acetyl) and OH groups occurred during heat treatment, despite the absence of any cross-linking agent. However, for the cross-linked samples, the plateau achieved is lower than that of XG_WF, meaning that the presence of cross-linking agent increases the cross-linking density, which is inversely proportional to the swelling capacity (Peppas, 1986). Indeed, WU of samples made with CA ranges from 490 % to 740 % and it decreases with the cross-linking agent content. The opposite behavior is instead observed for samples cross-linked with STMP. This can be attributed to the fact that, in addition to the cross-links, the reaction with STMP introduces more anionic charges into the XG chains. Therefore, the water uptake in STMP cross-linked hydrogels becomes greater due to the higher number of negative charges within the phosphorus species. Furthermore, the counter ions within these hydrogels, which neutralize the fixed charges on the polymer chains, lead to an increase of the osmotic pressure and result in a high swelling ratio (Shalviri et al., 2010; Tao et al., 2016). WU of these samples reaches plateau values ranging from 490 % to 700 %, i.e., lower than that

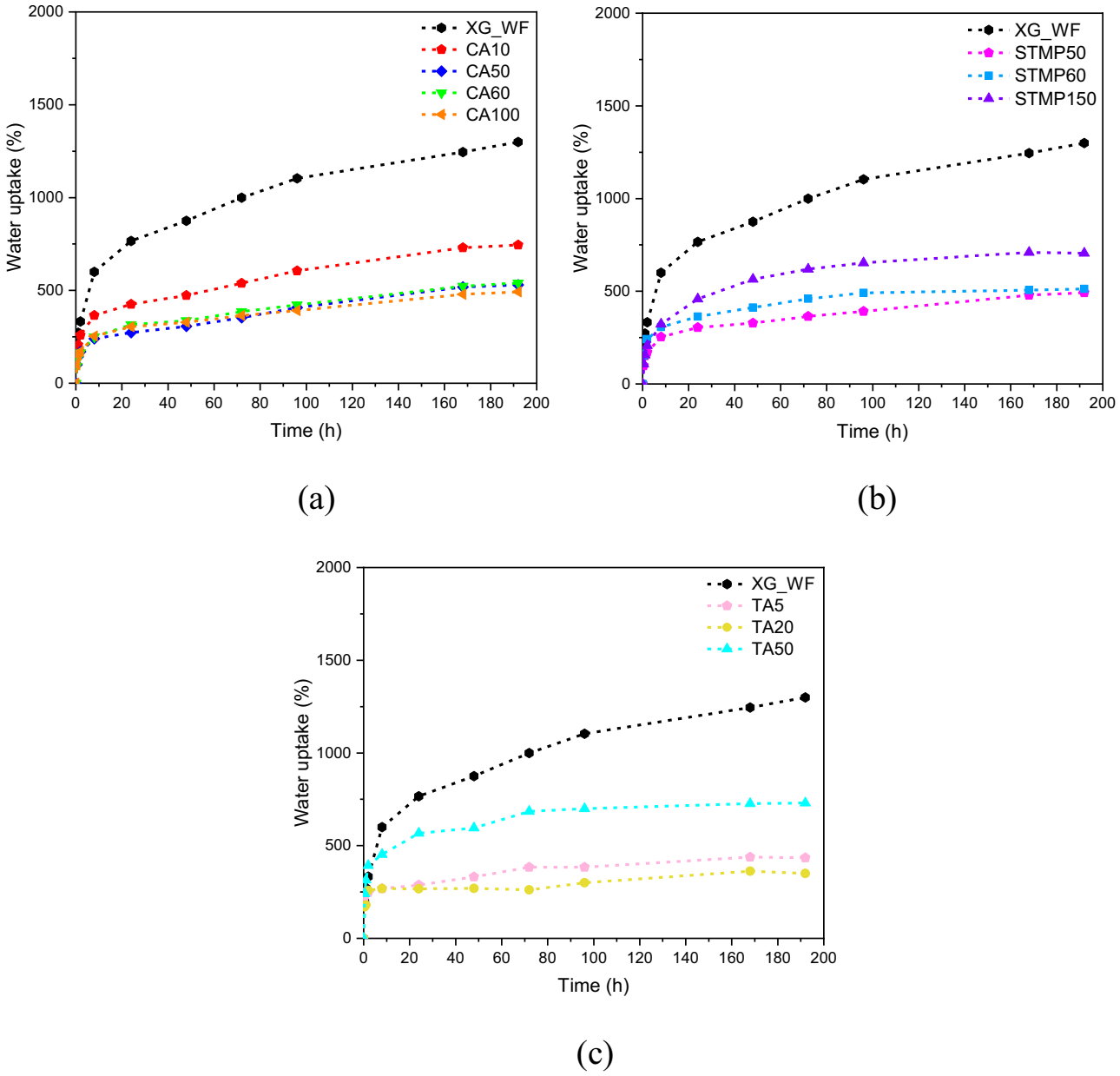

Fig. 4. Water absorption curves of XG_WF sample and hydrogels cross-linked with (a) CA, (b) STMP and (c) TA.

observed for CA cross-linked samples. For hydrogels cross-linked with TA, the increase of the cross-linking agent content leads to a higher concentration of hydrophilic groups in the hydrogel structure. Thus, the cross-linking density decreases with a consequent increase in water uptake and swelling (Ulu, Birhanlı, & Ateş, 2021). For these samples the WU ranges from 360 % to 800 %. Although most of the curves in the Fig. 4(a–c) have a parabolic trend, by fitting the data according to Equation (VI) it is possible to notice that the values of the diffusion coefficient n are lower than 0.5. This means that the diffusion mechanism that drives the water absorption is described as quasi-Fickian, and the water molecules pass through a preferential way inside interconnected pores of the hydrogel.

Table 3 reports the values of the final water uptake of the samples after multiple water absorption/desorption cycles. During the third cycle, the STMP cross-linked samples and most of the TA cross-linked hydrogels show instability and leakage due to excessive swelling, which lead in some cases to their breakage before reaching a plateau.

The first notable result is that WU of samples after the second absorption cycle is almost the double compared to the first one. This is related to the fact that, after the first cycle, part of the water soluble mass, mainly glycerine, is washed away. However, this is not a problem for the intended application of these materials, as the glycerine acts as a plasticiser and it has been introduced only to facilitate the sample preparation by dissolving the xanthan gum without the formation of lumps, and to make the TSCs flexible to ease their placement around the plant. Nevertheless, all samples are able to reach again an absorption plateau afters 8 days of immersion. In all cases the plateau value reached is lower than that of XG_WF sample (2800 %). Ultimate WU of samples cross-linked with CA is practically independent from the CA content, with values ranging from 1400 % to 1500 % after 8 days. For the STMP and TA cross-linked samples the values of WU after the second cycle are found to be independent from the concentration of cross-linking agent. From the results of the third absorption cycle it is possible to observe that the reference sample reaches an elevated WU value (3700 %), because of the rupture of the sample, of the continuous leaking of material and thus of the continuous absorption of water, which lead to the almost complete loss of the sample itself. Samples obtained with CA, on the other hand, are all able to resist a full third cycle of immersion and show noticeable stability. Final WU values are comparable to those obtained during second cycle, and range from 1550 % to 1800 %. From these tests, considering the need for a topsoil cover to have good WU ability and, most importantly, high stability after different water absorption/desorption cycles, CA50, CA60 and CA100 are found to be the most promising compositions for the intended application. No significant difference at 0.05 level can be found between these samples for all the cycles. This means that, for the amount of XG used, a threshold value of the degree of cross-linking has been reached, above which, no significant improvement in properties can be obtained. Also, TA5 should be kept into consideration due to its good WU behavior.

Table 3
Values of the final water uptake measured for the prepared hydrogels after multiple water absorption/desorption cycles.

Sample	WU (I cycle) (%)	WU (II cycle) (%)	WU (III cycle) (%)
XG_WF	1300 ± 71 a	2826 ± 217 a	3669 ± 567 a
CA10	744 ± 29 b	1569 ± 20 bc	1812 ± 108 b
CA50	530 ± 30 bc	1425 ± 23 b	1558 ± 61 b
CA60	540 ± 25 bc	1549 ± 80 bc	1662 ± 138 b
CA100	491 ± 33 c	1596 ± 29 bc	1730 ± 105 b
STMP50	486 ± 35 c	2535 ± 49 a	–
STMP60	513 ± 70 c	2082 ± 139 c	–
STMP150	704 ± 114 b	2772 ± 23 a	–
TA5	434 ± 74 c	1301 ± 202 bd	1904 ± 418 b
TA20	361 ± 23 c	875 ± 53 d	–
TA50	726 ± 188 b	1747 ± 516 b	–

Different letters in a column indicate that results are statistically different ($p < 0.05$).

3.4. Evaluation of the water vapor permeability

Values of WVP2 and WVP of the different xanthan/wood fibers based hydrogels, calculated according Equation (VII) and (VIII), are reported in Table 4 and compared with those of a commercial woven PP mulching film.

In general, the water-barrier properties of xanthan/wood fibers based hydrogels are rather poor due to the presence of hydrophilic groups, which increase the water absorption properties but also increase the water vapor permeability (Long, Zhang, Zhao, & Ruan, 2023). However, positive results can be seen by looking at the WVP2 values of the CA cross-linked samples, which are lower than that of XG_WF and comparable to that of the commercial woven PP mulch film. This can be explained by the fact that the cross-linking reaction between citric acid and XG reduces the amount of available hydrophilic groups in the structure and thus reduces the water vapor moving through the hydrogel structure, thus increasing the water barrier properties. However, the WVP values of the xanthan/wood fibers-based hydrogels are still one order of magnitude higher than that of the commercial product. This can be explained by the fact that the permeability is strongly influenced by the thickness of the sample (increasing the thickness, the WVP increases (Bertuzzi, Vidaurre, Armada, & Gottifredi, 2007)) and, in this case, the thickness of the commercial product is 10 times lower than that of the produced hydrogels. Furthermore, the presence of a plasticizer such as glycerol in the hydrogels increases the mobility of the polymer chains and thus further enhances the water vapor diffusion properties (Guilbert, Gontard, & Cuq, 1995). Samples cross-linked with STMP and TA show much higher WVP2 and WVP values with respect to the commercial mulching film, without any clear influence of the cross-linking agent content. This behavior can be explained by the high swelling tendency of these samples once in contact with water (Bertuzzi et al., 2007). For topsoil cover applications it would be important to have WVP values as low as possible, in order to limit the water evaporation rate from soil, as in the case of the commercial products. However, it is important to underline that the thickness of the hydrogels prepared in this work can be adjusted during the preparation phase in order to obtain the desired water vapor barrier properties.

3.5. Evaluation of the penetration resistance

Fig. 5 shows the results of penetration resistance tests performed on the xanthan/wood fibers based hydrogels and on the PP commercial film, expressed in terms of maximum load sustained by the samples.

It can be seen that for all the samples produced the maximum penetration load is between 12 N and 20 N, and that their penetration resistance is mainly determined by the formation of a network of wood fibres that confers stiffness to the hydrogels. Considering the standard deviations values, there is no substantial influence of the type and concentration of the cross-linking agent on the penetration resistance and, overall, there is no significant difference at 0.05 level between

Table 4
Values of WVP2 and WVP of the xanthan/wood fibers based hydrogels and of a commercial PP mulching film.

Sample	WVP2 × 10^{-6} ($g \bullet m^{-2} \bullet s^{-1} \bullet Pa^{-1}$)	WVP × 10^{-9} ($g \bullet m^{-1} \bullet s^{-1} \bullet Pa^{-1}$)
XG_WF	14.7 ± 0.4	37.5 ± 1.2
CA10	11.4 ± 0.3	32.2 ± 0.7
CA50	10.2 ± 0.3	30.7 ± 0.1
CA60	9.9 ± 0.1	29.0 ± 0.1
CA100	9.1 ± 0.1	27.7 ± 0.1
STMP50	13.7 ± 0.4	40.7 ± 1.3
STMP60	14.8 ± 0.5	31.0 ± 2.8
STMP150	12.0 ± 0.5	34.3 ± 1.2
TA5	14.8 ± 0.4	31.9 ± 0.2
TA20	17.2 ± 0.5	38.8 ± 0.4
TA50	15.0 ± 0.4	37.6 ± 0.5
PP film	8.1 ± 0.1	2.1 ± 0.1

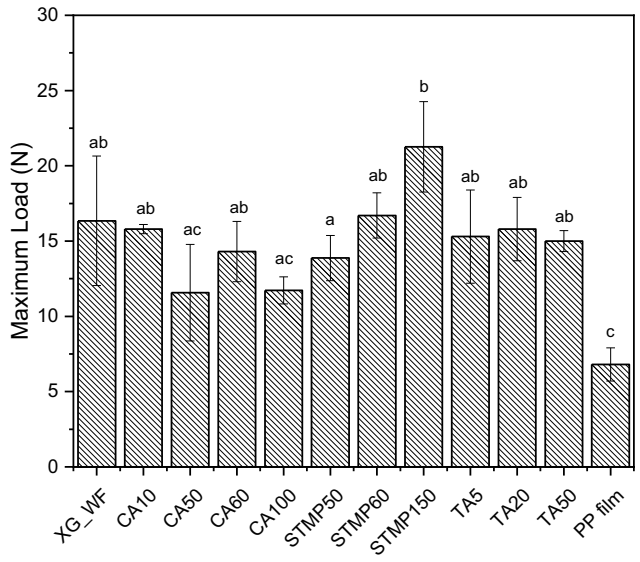

Fig. 5. Penetration resistance of the produced xanthan/wood fibers-based samples and of the commercial PP mulching film. Different letters indicate that results are statistically different ($p < 0.05$).

samples. The only significant difference ($p < 0.05$) cabin be found between STMP150 and CA50 and CA100. CA50 is characterized by high standard deviation, while the behavior of CA100 can be ascribed by its high CA content, which leads to a stiffening of the structure and a consequent lower penetration resistance. It is interesting to notice that most of the samples are statistically different ($p < 0.05$) with respect to the commercial PP woven film, which shows a mean penetration resistance of 6.8 N. This difference may be attributed to the much lower thickness of the PP commercial film. However, for the purpose of this test, i.e., the assessment of the ability of the TSCs to resist weed perforation, the absolute maximum penetration load should be considered, without any normalization. It is also important to underline that these penetration resistance values refer to dry samples which, in a practical topsoil cover application, would correspond to the initial condition in which the samples are placed around the plant. From this point on, the samples will be subjected to substantial variations of the environmental conditions (i.e., temperature, humidity, UV radiation) that may alter the structure of the hydrogel, causing swelling and thus changing its mechanical properties. Therefore, further investigations will be needed to study the mechanical resistance of these hydrogels under different environmental conditions.

3.6. Weather conditioning in external environment

Area loss and residual mass experienced by the hydrogels with optimized composition (i.e., CA60 and TA5) in weather conditioning tests are reported in Table 5.

It can be seen that the area loss does not decrease steadily over time, but it can also increase. This is due to the fact that, in the presence of rainfall, the materials absorb water and swell, increasing their volume.

Table 5
Results of outside weather conditioning tests after 1, 2 and 7 months on the prepared hydrogels with optimized composition.

Sample	A_L 1 month (%)	A_L 2 months (%)	A_L 7 months (%)	Residual Mass 7 months (%)
CA60	22.1 ± 1.1	15.4 ± 2.3	50.7 ± 8.0	36.4 ± 6.6 a
TA5	22.2 ± 1.2	29.2 ± 2.1	46.5 ± 8.3	57.6 ± 8.9 b

Different letters in a column indicate that results are statistically different ($p < 0.05$).

In general, the samples show good stability after 2 months, as it has been already seen after multiple cycles of water absorption and desorption (see Section 3.3), due to the presence of the cross-linking agents. During the test, the samples show some warping and deformation, but substantially maintain their original shape. This is due to the presence of the network of long wood fibers (9–30 mm length) in the hydrogels, which limits shrinkage during drying periods. The values of residual mass indicate that samples underwent biodegradation, which is more prominent for the CA60 sample which shows a greater mass loss at the end of the test compared to TA5 sample ($p < 0.05$). Further biodegradation assays and standardized tests will be planned in order to investigate more deeply this aspect. The development of fully biodegradable topsoil covers is of paramount importance to overcome the problems of end-of-use removal of commercial plastic mulch films. By tuning the size of TSCs and the cross-linking agent content, it would be possible to tailor the biodegradation time of the samples. In agricultural applications the maximum time required for the complete biodegradation of TSCs is only few months (seasonal planting), while in forestry applications their service time could be longer (1 or 2 years). It is also important to note that the growth of vegetation was completely inhibited in the area below the samples for the first 3 months, while grasses and weeds only grew in the area between them. After 7 months, due to weather effects and the biodegradation of materials, different weed filaments were able to perforate the samples.

4. Conclusions

In this work, multifunctional bio-based and biodegradable hydrogels constituted of xanthan gum and wood fibers were developed with the aim to produce novel eco-sustainable topsoil covers for the agricultural and forestry sectors, able to support plant growth and increase their survival rate, especially under drought conditions. Different cross-linking agents, such as citric acid, sodium trimetaphosphate and tannic acid, were added in different concentrations to obtain cross-linked hydrogels with different physical properties. Water absorption tests highlighted the capacity of the developed hydrogels to effectively absorb water after multiple absorption/desorption cycles, especially in samples cross-linked with citric acid. These hydrogels also exhibited water vapor permeance values comparable to that of a commercial plastic mulching film along with good penetration resistance, an important property for mulching films to inhibit weed growth. On the basis of the results of outdoor weathering conditioning tests, it was assessed that citric acid cross-linked hydrogels manifested a good stability after 2 months and suitable biodegradability after 7 months, with a final mass loss of 63.6 %. An important consideration concerns the economic feasibility of the produced materials, as the current market price of xanthan gum (at high purity level) is still high and limits their applicability. However, considering that high purity materials are generally not required for these applications and in view of the future industrial upscaling of the products, it is expected that the cost will become more affordable in the near future.

Funding

This project has received funding from the European Union's Horizon 2020 Research and Innovation Program within the project ONE-Forest: A Multi-Criteria Decision Support System for A Common Forest Management to Strengthen Forest Resilience, harmonize Stakeholder Interests and Ensure Sustainable Wood Flows (Grant Agreement No 101000406).

CRediT authorship contribution statement

Alessandro Sorze: Writing – review & editing, Writing – original draft, Validation, Software, Methodology, Investigation, Formal analysis, Data curation, Conceptualization. **Francesco Valentini:** Writing –

review & editing, Validation, Methodology, Investigation, Formal analysis, Conceptualization. **Matteo Burin Mucignat:** Writing – review & editing, Software, Investigation, Formal analysis, Data curation. **Alessandro Pegoretti:** Writing – review & editing, Visualization, Resources, Project administration, Funding acquisition. **Andrea Dorigato:** Writing – review & editing, Visualization, Supervision, Resources, Project administration, Funding acquisition.

Declaration of competing interest

The authors declare that they have no known competing financial interests or personal relationships that could have appeared to influence the work reported in this paper.

Data availability

Data will be made available on request.

References

Abrusci, C., Pablos, J. L., Corrales, T., López-Marín, J., Marín, I., & Catalina, F. (2011). Biodegradation of photo-degraded mulching films based on polyethylenes and stearates of calcium and iron as pro-oxidant additives. *International Biodeterioration & Biodegradation, 65*(3), 451–459.

Abu Elella, M. H., Goda, E. S., Gab-Allah, M. A., Hong, S. E., Pandit, B., Lee, S., Gamal, H., Rehman, A., & Yoon, K. R (2021). Xanthan gum-derived materials for applications in environment and eco-friendly materials: A review. *Journal of Environmental Chemical Engineering, 9*(1), Article 104702.

Aznar-Sánchez, J. A., Piquer-Rodríguez, M., Velasco-Muñoz, J. F., & Manzano-Agugliaro, F. (2019). Worldwide research trends on sustainable land use in agriculture. *Land Use Policy, 87*, Article 104069.

Becker, A., Katzen, F., Pühler, A., & Ielpi, L. (1998). Xanthan gum biosynthesis and application: A biochemical/genetic perspective. *Applied Microbiology and Biotechnology, 50*(2), 145–152.

Berninger, T., Dietz, N., & Gonzalez Lopez, O. (2021). Water-soluble polymers in agriculture: Xanthan gum as eco-friendly alternative to synthetics. *Microbial Biotechnology, 14*(5), 1881–1896.

Bertuzzi, M. A., Vidaurre, E. C., Armada, M., & Gottifredi, J. (2007). Water vapor permeability of edible starch based films. *Journal of Food Engineering, 80*(3), 972–978.

Briassoulis, D., & Giannoulis, A. J. P. T. (2018). Evaluation of the functionality of bio-based food packaging films. *Polymer Testing, 69*, 39–51.

Bueno, V. B., Bentini, R., Catalani, L. H., & Petri, D. F. (2013). Synthesis and swelling behavior of xanthan-based hydrogels. *Carbohydrate Polymers, 92*(2), 1091–1099.

Chang, I., Im, J., Prasidhi, A. K., & Cho, G.-C. (2015). Effects of Xanthan gum biopolymer on soil strengthening. *Construction and Building Materials, 74*, 65–72.

Chang, I., Lee, M., Tran, A. T. P., Lee, S., Kwon, Y.-M., Im, J., & Cho, G.-C. (2020). Review on biopolymer-based soil treatment (BPST) technology in geotechnical engineering practices. *Transportation Geotechnics, 24*, Article 100385.

Dennis, E. S., Dolferus, R., Ellis, M., Rahman, M., Wu, Y., Hoeren, F. U., Grover, A., Ismond, K. P., Good, A. G., & Peacock, W. J. (2000). Molecular strategies for improving waterlogging tolerance in plants. *Journal of Experimental Botany, 51*(342), 89–97.

Foley, J. A., DeFries, R., Asner, G. P., Barford, C., Bonan, G., Carpenter, S. R., Chapin, F. S., Coe, M. T., Daily, G. C., & Gibbs, H. K. (2005). Global consequences of land use. *Science (New York, N.Y.), 309*(5734), 570–574.

Gao, X., Xie, D., & Yang, C. (2021). Effects of a PLA/PBAT biodegradable film mulch as a replacement of polyethylene film and their residues on crop and soil environment. *Agricultural Water Management, 255*, Article 107053.

Garcıa-Ochoa, F., Santos, V., Casas, J., & Gómez, E. (2000). Xanthan gum: Production, recovery, and properties. *Biotechnology Advances, 18*(7), 549–579.

Guilbert, S., Gontard, N., & Cuq, B. (1995). Technology and applications of edible protective films. *Packaging Technology and Science, 8*(6), 339–346.

Jang, H. Y., Zhang, K., Chon, B. H., & Choi, H. J. (2015). Enhanced oil recovery performance and viscosity characteristics of polysaccharide xanthan gum solution. *Journal of Industrial Engineering Chemistry, 21*, 741–745.

Kasirajan, S., & Ngouajio, M. (2012). Polyethylene and biodegradable mulches for agricultural applications: A review. *Agronomy for Sustainable Development, 32*, 501–529.

Kayserilioğlu, B.Ş., Bakir, U., Yilmaz, L., & Akkaş, N. J. B.t. (2003). Use of xylan, an agricultural by-product, in wheat gluten based biodegradable films: mechanical, solubility and water vapor transfer rate properties. *Bioresource Technology, 87*(3), 239–246.

Langer, R. S., & Peppas, N. A. (1981). Present and future applications of biomaterials in controlled drug delivery systems. *Biomaterials, 2*(4), 201–214.

Li, Y., Zhang, D., Ash, J., Jia, X., Leone, A., & Templeton, A. (2019). Mechanism and impact of excipient incompatibility: Cross-linking of Xanthan gum in pediatric powder-for-suspension formulations. *Journal of Pharmaceutical Sciences, 108*(11), 3609–3615.

Long, J., Zhang, W., Zhao, M., & Ruan, C.-Q. (2023). The reduce of water vapor permeability of polysaccharide-based films in food packaging: A comprehensive review. *Carbohydrate Polymers, 321*, 1–19.

Maiti, S., Maji, B., & Yadav, H. (2023). Progress on green crosslinking of polysaccharide hydrogels for drug delivery and tissue engineering applications. *Carbohydrate Polymers, 326*, 1–28.

Menossi, M., Cisneros, M., Alvarez, V. A., & Casalongué, C. (2021). Current and emerging biodegradable mulch films based on polysaccharide bio-composites. A review. *Agronomy for Sustainable Development, 41*(4), 1–27.

Merino, D., Gutiérrez, T. J., Mansilla, A. Y., Casalongué, C. A., & Alvarez, V. A. (2018). Critical evaluation of starch-based antibacterial nanocomposites as agricultural mulch films: Study on their interactions with water and light. *ACS Sustainable Chemistry & Engineering, 6*(11), 15662–15672.

Merino, D., Zych, A., & Athanassiou, A. (2022). Biodegradable and biobased mulch films: highly stretchable PLA composites with different industrial vegetable waste. *ACS Applied Materials Interfaces, 14*(41), 46920–46931.

Mirzabaev, A., Wu, J., Evans, J., García-Oliva, F., Hussein, I. A. G., Iqbal, M. H., Kimutai, J., Knowles, T., Meza, F., Nedjraoui, D., Tena, F., Türkeş, M., Vázquez, R. J., & M, W (2019). Desertification. In climate change and land: An IPCC special report on climate change, desertification, land degradation, sustainable land management, food security, and greenhouse gas fluxes in terrestrial ecosystems (Vol. 3, pp. 249–343).

Norton, M. R., Malinowski, D. P., & Volaire, F. (2016). Plant drought survival under climate change and strategies to improve perennial grasses. A review. *Agronomy for Sustainable Development, 36*(2), 1–15.

Patel, J., Maji, B., Moorthy, N., & Maiti, S. (2020). Xanthan gum derivatives: review of synthesis, properties and diverse applications. *RSC Advances, 10*(45), 27103–27136.

Peppas, N. A. (1986). *Hydrogels in medicine and pharmacy, 1*. Boca Raton, FL: CRC press.

Prigent, O., Wynn Owen, P., Homrich Hickmann, M., Bryan, K., Caruda Ruiz, A., & Huth, J. (2018). Combating desertification in the EU: A growing threat in need of more action. *European Court of Auditors, 33*, 65.

Qi, Y., Yang, X., Pelaez, A. M., Huerta Lwanga, E., Beriot, N., Gertsen, H., Garbeva, P., & Geissen, V. (2018). Macro- and micro- plastics in soil-plant system: Effects of plastic mulch film residues on wheat (Triticum aestivum) growth. *Science of the Total Environment, 645*, 1048–1056.

Russo, R., Malinconico, M., & Santagata, G. (2007). Effect of cross-linking with calcium ions on the physical properties of alginate films. *Biomacromolecules, 8*(10), 3193–3197.

Santos, T. M., Men de Sá Filho, M. S., Silva, E.d. O., da Silveira, M. R., de Miranda, M. R. A., Lopes, M. M., & Azeredo, H. M. J. F.c. (2018). Enhancing storage stability of guava with tannic acid-crosslinked zein coatings. *Food Chemistry, 257*, 252–258.

Shalviri, A., Liu, Q., Abdekhodaie, M. J., & Wu, X. Y. (2010). Novel modified starch–xanthan gum hydrogels for controlled drug delivery: Synthesis and characterization. *Carbohydrate Polymers, 79*(4), 898–907.

Sorze, A., Valentini, F., Dorigato, A., & Pegoretti, A. (2023). Development of a xanthan gum based superabsorbent and water retaining composites for agricultural and forestry applications. *Molecules (Basel, Switzerland), 28*(4), 1952.

Sorze, A., Valentini, F., Smolar, J., Logar, J., Pegoretti, A., & Dorigato, A. (2023). Effect of different cellulose fillers on the properties of xanthan-based composites for soil conditioning applications. *Materials, 16*(23), 7285.

Steinmetz, Z., Wollmann, C., Schaefer, M., Buchmann, C., David, J., & Tröger, J. (2016). Plastic mulching in agriculture. Trading short-term agronomic benefits for long-term soil degradation? *Science of the Total Environment, 550*, 690–705.

Tao, Y., Zhang, R., Xu, W., Bai, Z., Zhou, Y., & Zhao, S. (2016). Rheological behavior and microstructure of release-controlled hydrogels based on xanthan gum crosslinked with sodium trimetaphosphate. *Food Hydrocolloids, 52*, 923–933.

Thombare, N., Mishra, S., Siddiqui, M. Z., Jha, U., Singh, D., & Mahajan, G. R. (2018). Design and development of guar gum based novel, superabsorbent and moisture retaining hydrogels for agricultural applications. *Carbohydrate Polymers, 185*, 169–178.

Tian, Y., & Wang, J. H. (2020). Polyhydroxyalkanoates for biodegradable mulch films applications. *Sustainability & Green Polymer Chemistry Volume 2: Biocatalysis and Biobased Polymers* (pp. 145–160). ACS Publications.

Ulu, A., Birhanlı, E., & Ateş, B. (2021). Tunable and tough porous chitosan/β-cyclodextrin/tannic acid biocomposite membrane with mechanic, antioxidant, and antimicrobial properties. *International Journal of Biological Macromolecules, 188*, 696–707.

Vatanpour, V., Gul, B. Y., Zeytuncu, B., Korkut, S., İlyasoğlu, G., Turken, T., Badawi, M., Koyuncu, I., & Saeb, M. R. (2022). Polysaccharides in fabrication of membranes: A review. *Carbohydrate Polymers, 281*, Article 119041.

Wahyono, T., Astuti, D. A., Gede Wiryawan, I. K., Sugoro, I., & Jayanegara, A. (2019). Fourier transform mid-infrared (FTIR) spectroscopy to identify tannin compounds in the panicle of sorghum mutant lines. *IOP Conference Series: Materials Science and Engineering, 546*(4), 1–7.

Wang, J., Lv, S., Zhang, M., Chen, G., Zhu, T., Zhang, S., Teng, Y., Christie, P., & Luo, Y. (2016). Effects of plastic film residues on occurrence of phthalates and microbial activity in soils. *Chemosphere, 151*, 171–177.

Yang, N., Sun, Z.-X., Feng, L.-S., Zheng, M.-Z., Chi, D.-C., Meng, W.-Z., Hou, Z.-Y., Bai, W., & Li, K.-Y. (2015). Plastic film mulching for water-efficient agricultural

applications and degradable films materials development research. *Materials and Manufacturing Processes, 30*(2), 143–154.
Zhang, D., Liu, H.-b., Hu, W.-l., Qin, X.-h., Yan, C.-r., & Wang, H.-y. (2016). The status and distribution characteristics of residual mulching film in Xinjiang, China. *Journal of Integrative Agriculture, 15*(11), 2639–2646.
Zhao, Y., Qiu, J., Xu, J., Gao, X., & Fu, X. (2017). Effects of crosslinking modes on the film forming properties of kelp mulching films. *Algal Research, 26*, 74–83.